POTASSIUM IODIDE POTENTIATED PHOTODYNAMIC INACTIVATION OF ENTEROCOCCUS FAECALIS USING TOLUIDINE BLUE: COMPARATIVE ANALYSIS, PHOTOTHERMAL EFFECT, AND POST-TREATMENT BIOFILM FORMATION STUDY

by

Sahand A.Ghaffari

B.Sc., Physics, Boğaziçi University, 2016

Submitted to the Institute of Biomedical Engineering
in partial fulfillment of the requirements
for the degree of
Master of Science
in
Biomedical Engineering

Boğaziçi University
2018

POTASSIUM IODIDE POTENTIATED PHOTODYNAMIC INACTIVATION OF ENTEROCOCCUS FAECALIS USING TOLUIDINE BLUE: COMPARATIVE ANALYSIS, PHOTOTHERMAL EFFECT, AND POST-TREATMENT BIOFILM FORMATION STUDY

APPROVED BY:

Prof. Dr. Murat Gülsoy .....
(Thesis Advisor)

Assoc. Prof. Dr. Bora Garipcan .....

Prof. Dr. Inci Çilesiz .....

DATE OF APPROVAL: May 21 2018

ACKNOWLEDGMENTS

I would like to thank thesis advisor Prof. Dr. Murat Gülsoy for his constant support and availability throughout the project. I am also thankful to Ayşe Sena Kabaş Sarp who walked me through experimental microbiology aspect of the work, and Mustafa Kemal Ruhi who provided assistance with statistical analysis part and offered suggestions on theoretical aspect of photodynamic therapy.

This work would not have been done in time without Assoc. Prof. Dr. Bora Garipcan's helpfulness in providing me with all missing materials/chemicals needed for the project. Members of both Biophotonics and Biomaterials labs are kindly acknowledged for providing help when asked for. This study was supported by Boğaziçi University research funds, BAP Project number 12744/17XD1. Finally, I wish to thank my wife Sevil, whose patience and moral support motivated me, and my parents who always stood by me unconditionally.

This thesis is dedicated to my beloved son Ferzan Sohrab.

ACADEMIC ETHICS AND INTEGRITY STATEMENT

I, Sahand A.Ghaffari, hereby certify that I am aware of the Academic Ethics and Integrity Policy issued by the Council of Higher Education (YÖK) and I fully acknowledge all the consequences due to its violation by plagiarism or any other way.

Name :

Signature:

Date:

ABSTRACT

POTASSIUM IODIDE POTENTIATED PHOTODYNAMIC INACTIVATION OF ENTEROCOCCUS FAECALIS USING TOLUIDINE BLUE: COMPARATIVE ANALYSIS, PHOTOTHERMAL EFFECT, AND POST-TREATMENT BIOFILM FORMATION STUDY

Antimicrobial Photodynamic Inactivation (aPDI) has recently gained interest as an alternative modality to fight pathogenic entities. Its effect can also be further enhanced by using certain inorganic salts. Here, the Potassium Iodide (KI) - mediated aPDI effect on Enterococcus faecalis using Toluidine Blue Ortho (TBO) as photosensitizer (PS) has been evaluated, and the Photothermal effect as well as subsequent Biofilm formation extent are accounted for. The comparative photoinactivation of TBO and TBO/KI on E.faecalis was investigated by quantifying surviving bacterial colonies after laser irradiation with 30,60,and 180 second exposure times and different PS/Potentiator concentrations. The degree of photothermal effect was measured by obtaining a temperature profile using thermocouple. The biofilm formation capability of E.faecalis was observed by calculating Optical Density (OD595) of samples 0, 24, 48, and 72 hours post- aPDI treatment. Scanning Electron Microscopy (SEM) was used as a qualitative measure of bacterial biofilm growth. More than 4 LOGS of photokilling was obtained for experimental groups with the highest PS/KI concentrations at 180 s exposure time. All KI-potentiated groups showed enhancement in aPDI effect when compared to non-potentiated counterparts. Moreover, an average temperature increase of about 2°C,with 180 s laser exposure, proved photothermal effect to be negligible. The degree of recurring biofilm for laser-treated groups also showed to be much less than that of control group, as confirmed by both OD595 measurement and SEM imaging.

Keywords: E.faecalis, TBO, aPDI, Biofilm, Potassium Iodide, Potentiator.

ÖZET

ENTEREOCOCCUS FAECALIS'IN TOLUIDIN BLUE KULLANILARAK POTASYUM İYODÜR ILE DOZU ARTTIRILMIŞ FOTODINAMIK İNAKTIVASYONU: KARŞILAŞTIRMALI ANALIZ, FOTOTERMAL ETKI VE UYGULAMA SONRASI BIYOFILM OLUŞUMUNUN İNCELENMESI

Bu çalışmada, patojen bakterileri yok edebilmek için alternatif bir yöntem olan Antimikrobiyal Fotodinamik Inaktivasyonunun (aPDI) etkisinin belirli inorganik tuzlar kullanılarak artırılması araştırılmıştır. Enterococcus faecalis bakterisi üzerinde fotosensitizan (PS) olarak Toluden Blue Ortho (TBO) ve tuz olarak Potasyum İyodür (KI) kullanılarak antimikrobiyal Fotodinamik İnaktivasyonu olgusu degerlendirilirken photothermal etki ve biyofilm oluşum derecesi de incelenmiştir. TBO ve TBO/KI'nın E.faecalis üzerindeki foto inaktivasyonları 30, 60 ve 180 saniye ısıma zamanları ve farklı PS / potansiyatör konsantrasyon grupları ile karşılaştırılıp, laser uygulamasından sonra hayatta kalan bakteri koloni sayıları ölçülerek araştırıldı. Işılçift kullanılarak sıcaklık profili elde edilerek fototermal etki derecesi ölçüldü. Antimikrobiyal fotodinamik tedaviden 0, 24, 48 ve 72 saat sonra E.faecalis'in biyofilm oluşumu kabiliyeti, Optik Yogunluk (OD595) hesaplanarak gözlendi. Bakteriyel biyofilm büyümesinin kalitatif değerlendirilmesi Taramalı Elektron Mikroskobu (SEM) kullanılarak yapıldı. En yüksek PS / KI konsantrasyonlarına sahip, 180 saniyeden fazla ışımaya maruz kalan örnek gruplarında, bakteri sayılarında 4 log 'dan yüksek düşüş elde edimistir. KI ile desteklenmis grupların tümü, desteklenmemiş gruplara oranla daha yüksek bir anti bakteriyel etki göstermistir. Bunun ile birlikte, 180 saniye ısımaya maruz kalan gruplarda yaklaşık olarak 2°C'lik bir ortalama sıcaklık artışı fototermal etkinin ihmal edilebilir oldugunu kanıtlamıştır. Laser ile tedavi edilen gruplarda,OD595 ölçümü ve SEM görüntüleme yöntemleri ile teyit edilerek, tekrarlayan biyofilmin derecesinin kontrol grubununkinden çok daha az oldugu gözlenmistir.

Anahtar Sözcükler: E. faecalis, TBO, aPDI, Biyofilm, KI, Potansiyatör.

TABLE OF CONTENTS

LIST OF FIGURES

LIST OF TABLES

LIST OF SYMBOLS

°C	Degrees Centigrade
s	Seconds
h	Hours
g	Grams
λ	Lambda
μM	Micro Molar
mM	Milli Molar
μm	Micro Meter
MW	Milli watt
μl	Micro Liter

LIST OF ABBREVIATIONS

RBC	Red Blood Cells
WBC	White Blood Cells
PDT	Photodynamic Therapy
aPDI	antimicrobial Photodynamic Inactivation
LASER	Light Amplification by Stimulated Emission of Radiation
PS	Photosensitizer
KI	Potassium Iodide
TBO	Toluidine Blue Ortho
ROS	Reactive Oxygen Species
G(+)	Gram positive bacteria
G(-)	Gram negative bacteria
HOMO	Highest Occupied Molecular Orbital
LUMO	Lowest Unoccupied Molecular Orbital
PTT	Photothermal Therapy
LED	Light Emitting Diode
UTI	Urinary Tract Infection
CO2	Carbon Dioxide
ATCC	American Type Culture Collection
BHI	Brain Heart Infusion
dH2O	Distilled water
PBS	Phosphate Buffer Solution
CW	Continuous Wave
CR	Concentration Range
G	Group (experimental)
CV	Crystal Violet
OD595	Optical Density (at 595 nm wavelength)
CFU	Colony Forming Unit
SEM	Scanning Electron Microscopy

TCP	Tissue Culture Plate
ANOVA	Analysis Of Variance
LOG	Logarithm
CLSM	Confocal Laser Scanning Microscope

1. INTRODUCTION

1.1 The path to fight against infection

In medical dictionaries, the term "infection" is translated as the process in which certain microorganisms (bacteria, fungi, viruses, or protozoa) invade the body and multiply, resulting in appearence of symptoms that include but are not limitted to: fever, nausea, diarrhea, anemia or low Red Blood Cell (RBC) count, dehydration, and loss of appetite [1, 2]. Any biological agent that causes infection is called a pathogen. Although many bacteria are naturally harmless, and can live in our body (mainly guts) without causing any issues, once their numbers get out of control, or if their location throughout the body gets displaced (e.g via bloodstream), the body's immune system acts upon them by means of increasing the number of leukocytes, also known as White Blood Cells (WBC) in order to restore this imbalance.

But when WBCs are outnumbered by pathogens, other means are necessary in order to aid the immune system to overcome the challenge. This fact was one of the major driving forces behind numerous endeavors in the past, which finally bore fruit when the first antimicrobial vaccines were successfully applied by Louis Pasteur in the 19th century to cure diseases like rabies and anthrax. Later, the discovery of penicillin by Alexander Fleming in 1928 opened the door for commercialization of antibiotics as the main antimicrobial drugs used in medicine, and this trend has continued on ever since. Today, the expansion in the antibiotics sales and consumption has reached such a grand scale that the pharmaceutical sector saw a 36% increase in manufacturing and sales only in the first decade of the 21st century [3].

The pandemics of infectious diseases is not new, and when considering the vast casualties that diseases such as plague, anthrax, tetanus, or pneumonia have brought to human population, together with the fact that the revolutionary success of the antibiotics has resulted in increase in average life expectancy and reduced mortality rates,

it is no surprise to suspect that the current trend of relying heavily on antibiotics will continue. But, there remains a question of whether antibiotics are in fact the most ideal choice in the battle against infections.

Although the discovery of antibiotics was a major milestone in the fight against infections, their limitations in dealing with recurrent pathogens have called the thoroughness of their use into question. Moreover, it is getting harder for the pharmaceutical industry to keep up with the demand to introduce better antibiotics to solve the pathogen resistance issue, having to face challenges such as financial incentives and regulatory procedures [4–6].

A major aspect of the developing suspicion in suitability of antibiotics comes from the rather complex resistance strategies and mechanisms that many pathogens are capable of developing. Bacteria, as the main pathogenic class, have been around on this planet much longer than we have, so it is not shocking to realize that they have developed many complex mechanisms to help them survive any unfavored environment. Recent studies on such mechanisms reveal there are at least four major ways in which bacteria develop resistance to antibiotics. A summary of these mechanisms are summarized in Figure 1.1.

1. Increasing the **impermeability** of cell walls: bacteria are capable of modifying their cell wall proteins, in order to form thicker cell walls [8].This is a strategy that works among both types of bacteria, Gram(+) and Gram(-), regardless of differences in bacterial cell walls between the two (G(-) bacteria have cell walls that are on average 10-15 nm thicker than G(+) bacteria).

2. Changing the **target site**: Bacteria can basically deceive antibiotics by providing them with wrong and useless binding sites (e.g. by enzymatic alteration of the binding site via addition of a methyl group) [9].

3. Pumping drug molecules out of their cell walls, via their **efflux pumps** [10].

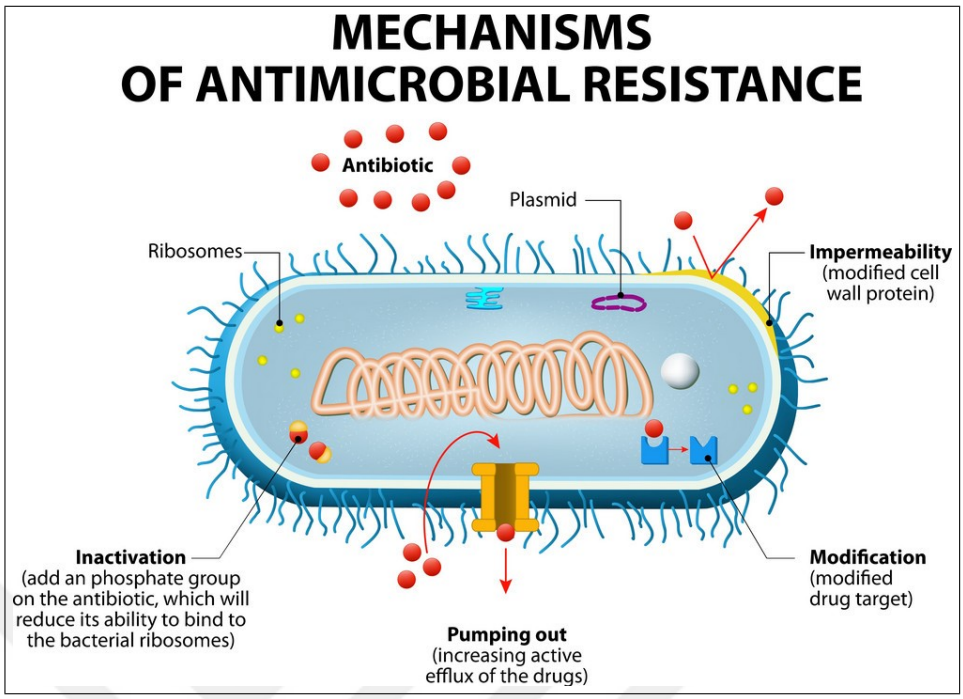

Figure 1.1 Mechanisms of Antibiotic Resistance by Bacteria [7].

4. **Inactivating** the antibiotics: bacteria are capable of protecting their ribosomes from being reached by drugs by means of attaching phosphate groups on the antibiotics molecules, which will eventually neutralize them [11].

Considering all these facts, it becomes evident that the search for alternative treatment options in battling infections should become a new scientific quest.

1.2 Photodynamic Therapy

One such alternatives is antimicrobial Photodynamic Therapy (aPDT). A typical PDT treatment involves introducing a photoreactive chemical substance called photosensitizer, usually denoted with (1PS) in its ground state, into body. When (1PS) absorbs light of a certain wavelength, it initially transitions into singlet excited state and this excited form (1PS*) then undergoes an electron spin conversion to its triplet excited state (3PS*), which can eventually transfer its energy to diatomic oxygen molecule which has triplet state as well, a transition that is quantum mechanically

allowed. This, upon conversion of triplet oxygen to singlet form, results in production of reactive oxygen species (ROS) in nearby media. The Oxygen molecular orbital shows that the ground state of molecular oxygen is in triplet state ($^3O_2$), while its excited and more reactive version ($^1O_2$) is in singlet state. The fact that the two electrons in the π-antibonding Highest Occupied Molecular Orbital (HOMO) couple together with opposite spins and leave a second π-antibonding Lowest Unoccupied Molecular Orbital (LUMO) empty implies less stability and higher reactivity for this species. Figure 1.2 demonstrates the molecular orbital representation of both triplet and singlet forms of oxygen.

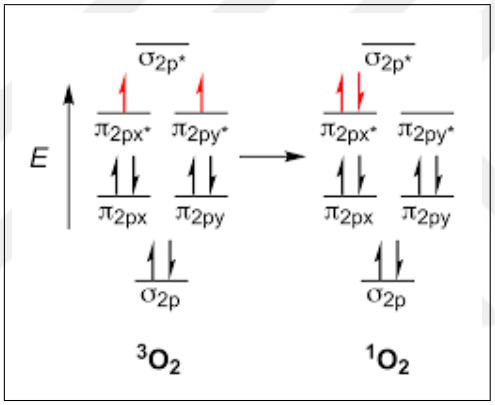

Figure 1.2 Molecular Orbital diagrams for triplet and singlet oxygen [12].

ROS generation during PDT is done via two possible pathways, known as Type I and Type II mechanisms. In type I, the (3PS*) reacts with the nearby media to produce free radicals (mainly $OH^{\bullet}$) while in type II , the (3PS*) transfers its energy to nearby oxygen molecules, thus converting them into reactive singlet oxygen($^1O_2$) molecules [13], and this reactive singlet oxygen then destroys any nearby malignancies due to its high chemical reactivity. Figure 1.3 shows a schematic diagram of a PDT mechanism of action.

Currently, PDT is used to treat both cancer and infectious diseases. For cancer treatment, PDT has been applied to cure esophageal cancer, dermatologic cutaneous

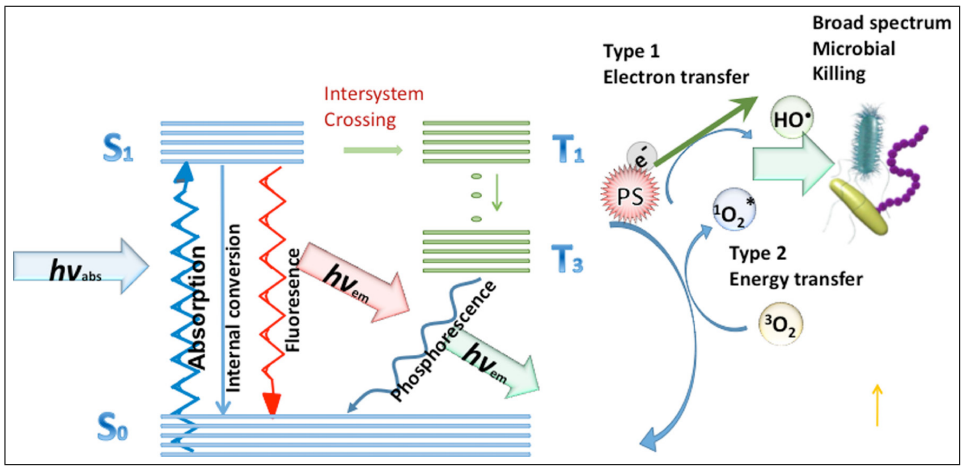

Figure 1.3 Jablonski diagrams for a conventional PDT procedure [14].

and subcutaneous cancers, and non-small cell lung cancer. In many countries, PDT procedures have become regular practice methods and have passed clinical trial stages (e.g. Brazil) while in others such as Turkey, medical practice of PDT has still remained at in-vitro or in-vivo animal model testings, with the exception of aesthetic dermatology practice.

In selecting the right PS and experimental parameters for a successful treatment, one important factor is the type of pathogen. Because of different cellular structures, Gram(+) and Gram(-) bacteria show different affinities towards PSs [15]. Among different groups of photosensitizers, phenothiazinium dyes, a group of cationic PSs, are capable of penetrating negatively charged cell walls of both Gram(+) and Gram(-) bacteria [16]. In this study, Toluidine Blue Ortho, a dye with no toxicity and with medical applications as vital staining substance [17] was selected. It has maximum absorption wavelength at $\lambda = 630$ nm, so it can be easily activated by any red laser. TBO can penetrate into cell walls of both types of bacteria. Figure 1.4 shows the chemical structure of TBO.

So far, there have been many studies to document the aPDI effect of various PSs on a wide range of pathogens. Nevertheless, it is always desirable and essntial to seek methods that would enhance the photoinactivation effect since depending on the degree

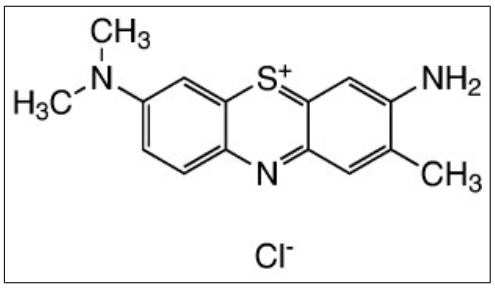

Figure 1.4 Chemical Structure of Toluidine Blue Ortho (TBO) [18].

of emergency in a treatment, it may be vital to accelerate the aPDI process. Thus, the idea of aPDI potentiation has started to attract attention in recent past. Some species with possible potentiation effect on bactericidal PDT are azide salts, halogen-bearing inorganic salts, or other naturally occuring compounds such as curcumin [19–21]. For the purpose of this study, potassium iodide (KI), a non-toxic inorganic salt that has been proven to exhibit antibacterial activities [22] was selected and its potentiation extent on aPDI effect of TBO on *Enterococcus faecalis* was analysed and compared with non-potentiated aPDI.

The bacteria of choice for this study, *Enterococcus faecalis*, is among the most common human pathogens. *E.faecalis* normally lives in the gastrointestinal system without causing harm, but in case of its transport and localisation into bloodstream, or via external acquisition, it can turn pathogenic. Its main target areas are the oral cavities and urinary tract environments [23–26]. Although the bacterial strains obtained from clinical subjects are proven to be more aggressive, for this thesis work, a reference strain of *E.faecalis* was obtained since the scope of the study was selected for an in-vitro analysis.

1.3 Photothermal effect

The main mechanism of action behind PDT is the photochemical effect. However, another aspect of treating illnesses in photomedicine is inducing a Photothermal effect near the target tissue. This is known as Photothermal Therapy (PTT). In PTT,

the increase in temperature induced by presence of a light source is the main principle behind elimination of malignancies. The light source, just as in the case of PDT, for a PTT session can be an arc lamp, laser system, or LED light source. Depending on the tissue type or the nature of medical problem, the physician can choose to apply either PDT, PTT, or a combination of the two, which results in a synergistic effect. As a matter of fact, many studies have focused on developing platforms using nanotechnology in order to combine the effects of the two methods, mainly in cancer therapy [27, 28], with some antibacterial work being done as well [29].

Since applying laser for extended periods of time can result in temperature increase in the nearby tissues, it is crucial to investigate the degree of involvement of photothermal effect during aPDI experiments. During this thesis work, some experimental groups were exposed to laser for up to a few minutes, so temperature profiling measures could be set up in order to monitor the effect of temperature.

1.4 Biofilm formation

Another important aspect of dealing with infections is biofilm formation. Biofilms form when planktonic bacteria attach to available surfaces in their environment and begin to form a layer. This structure allows them to form a sophisticated matrix, that enables more efficacious uptake of nutrients, via formation of a polymeric layer called the Extracellular Polymeric Substance (EPS) [30], and greater resistance to antibiotics [31]. Thus, a successful methodolgy to combat bacteria must be able to address biofilm formation. In the case of *E.faecalis*, it is capable of developing resistance to antibiotics by forming biofilm, and these biofilm communities are so strong that they even develop resistance to Vancomycin, a powerful antibiotic known as the drug of last resort. Although many studies have tried to erradicate *E.faecalis* biofilms using aPDI [25, 32], there is a need to account for the degree of post-treatment biofilm formation as well, as recurrence of biofilms can be a major concern.

One of the medical fields in which presence and recurrence of biofilm is an issue is Urology [33]. The presence of many toxins in the urether and bladder is a major cause of recurrence of infections in the urinary tract. Many patients with urologic problems have to use external means such as catheters or urinary stents to help them overcome malfunctions of the urologic organs. These malfunctions can be due to having kidney Stones, gallbladder Stones, tumors of the bladder, or Urinary Tract Infection (UTI). In many cases, and especially with older patients, devices such as stents are inserted inside the body, and depending on the need, they may be kept inside body for periods of time ranging from weeks to months. A major drawback in this situation is a phenomenon known as the encrustation of uretheral stents. Encrustation occurs when bacterial biofilms start to attach and form communities around both external and internal surfaces of the stent. This can cause acceleration of UTI, severe patient discomfort, and may contribute to higher morbidity rates [34]. Figure 1.5 shows images of a type of stent called double J (or J-J) uretheral stent and biofilm encrustation on its surface.

For the above mentioned reasons, this study was further extended to monitor post-treatment biofilm formation for a short period of time.

Figure 1.5 Image of biofilm encrusted J-J uretheral stent [35].

2. MATERIALS AND METHODS

2.1 Bacterial strain and media condition

A reference strain (American Type Culture Collection) of *E.faecalis* (ATCC19433) was used and bacterial strains were isolated in Brain Heart Infusion (BHI) solution and incubated under aerobic environment supplemented with 5% CO_2 at 37°C. *E.faecalis*-containing liquid growth media were renewed using fresh BHI every 72 hours.

2.2 Photosensitizer and Potentiator solutions

TBO (Sigma-Aldrich Corp., St. Louis, MO, USA) in powder form was used, and a stock solution with concentration of 100 μM was prepared in sterile dH2O , and was then filtered using 0.22 μm syringe filter (Corning Ltd) to ensure elimination of any bacterial contamination. The filtered stock solution was then stored in dark at 4 °C for two weeks. A 100 mM stock solution of KI (Sigma-Aldrich Corp., St. Louis, MO, USA) was prepared using sterile dH2O, and was stored at room temperature for one week.

2.3 Light source

A 635 nm diode laser system (Thorlabs Inc,Newton, NJ, USA) was used in continuous wave (CW) mode with output laser power of 300 mW. The radiation distance from tip of the fiber optic to bottom of the multi-well plates was measured to be 10.5 cm, and the beam diameter of 1.3 cm resulted in fluences of 6.8, 13.6, and 40.9 J/cm^2 for three irradiation intervals of 30, 60, and 180 s respectively. Figure 2.1 shows the

laser setup for the experiments.

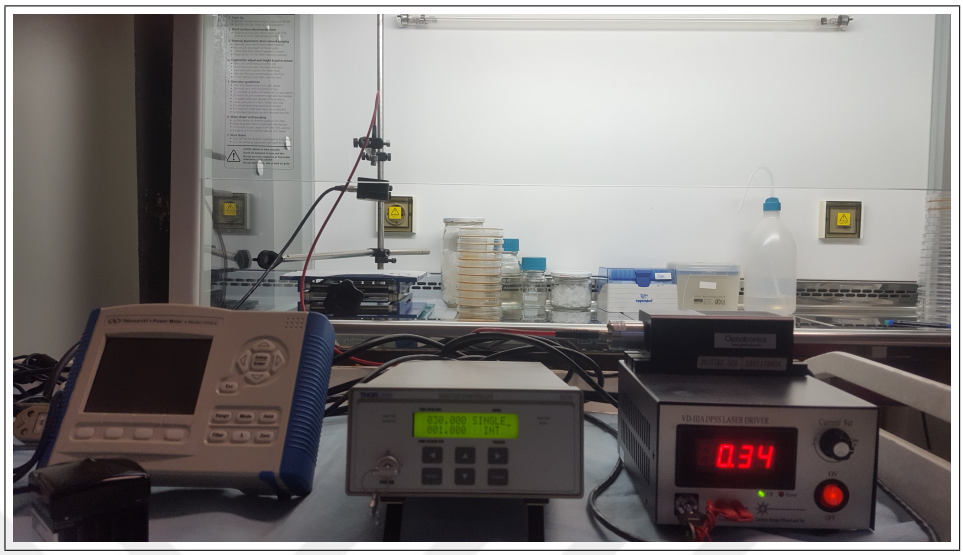

Figure 2.1 Laser device setup for the experiments. Left to right: Power meter, Shutter controller, Current adjuster. Fiber optic output is seen at the back.

2.4 aPDI Experiments

All experiments were performed under a Class II Biosafety cabin to ensure working under sterile conditions. 48-well plates (Crystal-grade polystyrene, SPL life sciences, South Korea) were used for experiments, as the diameter of wells matched well with radiation beam diameter, thus maximizing the irradiated surface covered. Sterile phosphate buffer solution (PBS) at pH=7.2 was used in order to suspend bacterial strains.

aPDI parameters such as light dose (300 mW), final PS/KI concentrations, and exposure times (30/60/180 s) were selected according to preliminary studies and previous work done by our group [36]. To see the aPDI extent at different concentrations, the PS and KI concentration ranges of one order of magnitude higher than before were also selected, yielding the following four concentration ranges (CR) listed in table 2.1.

In addition, in order to have a complete comparative measure of bactericidal

Table 2.1
Experimental concentration ranges and their respective components.

Concentration Range (CR)	**TBO (μM)**	**KI (mM)**
CR1	1	1
CR2	1	10
CR3	10	1
CR4	10	10

effect, aPDI experiments were carried out with the following experimental Groups (G) for each of the above-mentioned CR. These groups are listed on table 2.2.

Table 2.2
Experimental Groups and their descriptions and labels.

Groups (G)	**Description**	**Label**
G1	Negative control	(L-PS-KI-)
G2	Positive control (dark toxicity)	(L-PS+KI-)
G3	Positive control (KI only)	(L-PS-KI+)
G4	Positive control (dark toxicity with KI)	(L-PS+KI+)
G5	Laser only	(L+PS-KI-)
G6	Laser and KI only	(L+PS-KI+)
G7	Normal PDT	(L+PS+KI-)
G8	Potentiated PDT	(L+PS+KI+)

After addition of PS, the plates were incubated for 30 minutes at 37 °C to allow for localization of PS inside bacterial cells. Although some studies have suggested centrifugation and resuspension of well contents after incubation to remove non-localized PS from the liquid media, in these experiments, this step was deliberately skipped as it is possible that ROS generated in extracellular environment via excited PS also contribute to aPDI [37]. KI was added right before laser irradiation. The same procedure was performed for sets with 30, 60, and 180 s irradiation times. After lasing, 100 μl aliquots from each experimental group was taken and serially diluted in PBS up to

10-5 dilution factors. 20 μl aliquots were then taken and spread on solid agar plates and incubated at 37 °C for 48 hours before CFU counting. Figures 2.2 and 2.3 show an image of the aPDI experiment, and top view of a well plate containing experimental groups.

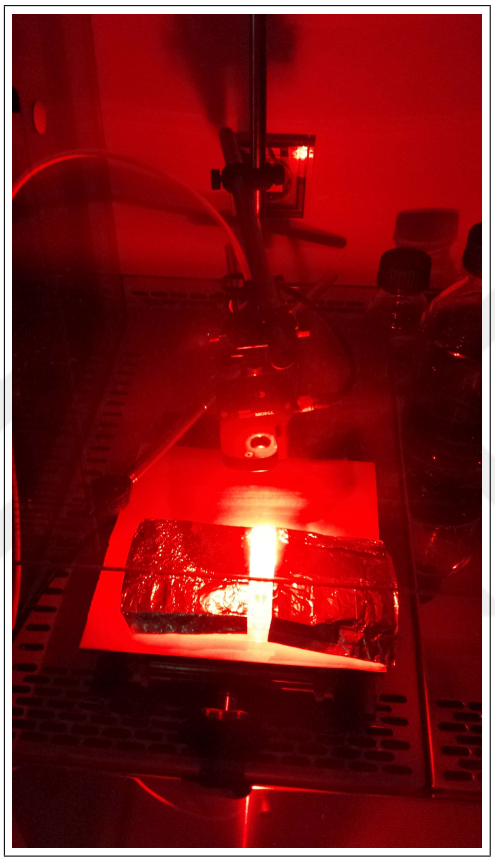

Figure 2.2 Image of an aPDI procedure.

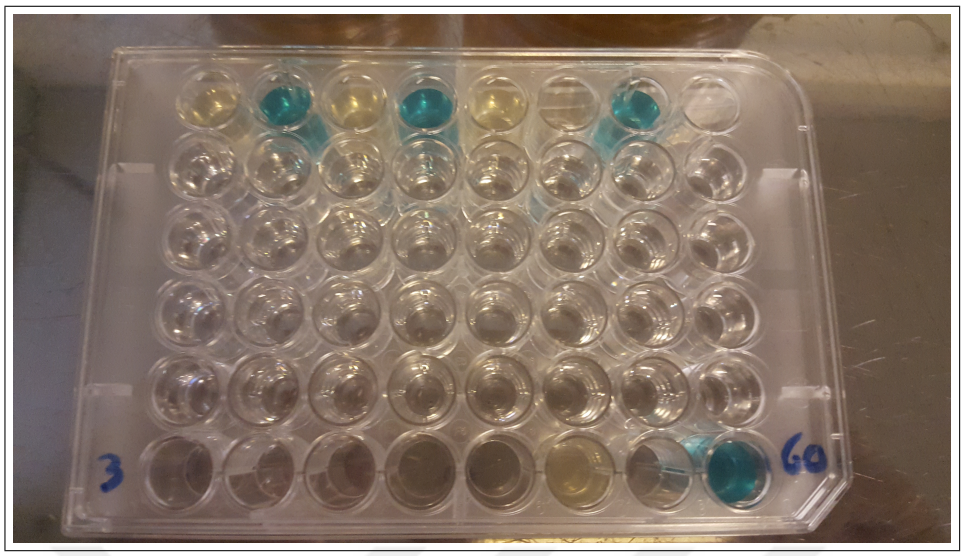

Figure 2.3 Top view of an experiment 48 well-plate .

2.5 Photothermal effect studies

Temperature increase was measured for a period of 180 s during laser irradiation in order to investigate its role in aPDI experiments. 48-well plates were used with PBS as the media, and a hypodermic needle microprobe thermocouple (MT-29/1,Physitemp) was inserted at the bottom of wells. A type T thermocouple thermometer (BAT-10, Physitemp) was used to record temperature profile at 10 s intervals. The experiments were repeated at least three times. Figure 2.4 shows the experimental setup, with photothermal measurement unit included.

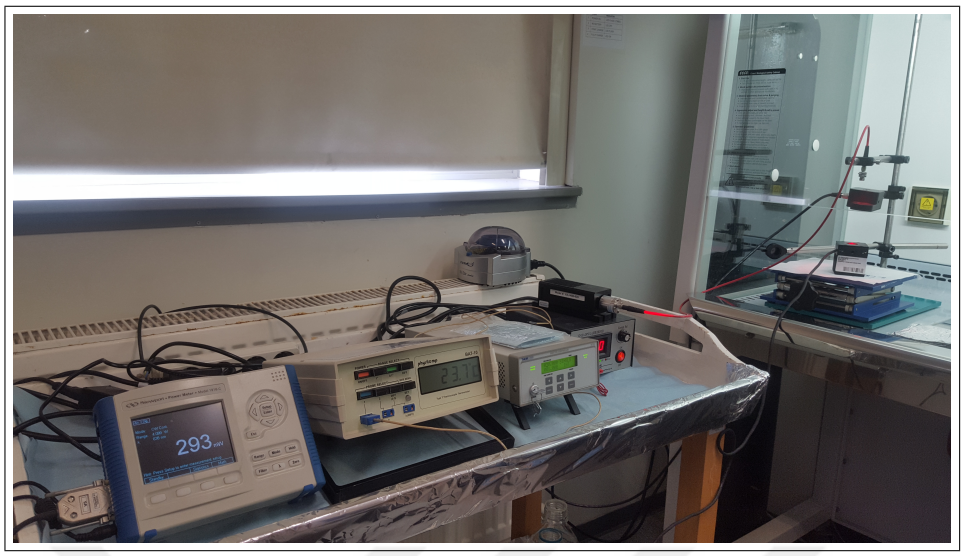

Figure 2.4 Photothermal effect measurement setup. Second from left: Thermometer device, coupled with thermocouple.

2.6 Post-treatment biofilm formation evaluation

Crystal Violet (CV) assay was used as a method to quantify biofilm formation after aPDI treatments by measuring Optical Density (OD_{595}) of samples at four different precise time intervals of 0, 24, 48, and 72 hours. For the sake of simplicity, sets with the most effective groups (CR4, 180 s) were used, and wells containing groups G1, G7, and G8 were selected for post-treatment biofilm analysis. After the experiments, contents of each well were devided into four parts, and one aliquot remained in the original experimental plate to be used for OD_{595} measurement at t = 0 h, while the other three aliquots were placed in three different plates for analysis at the other three time points (24,48,72 h). The quantification protocol by O'Toole et al. [38] was used with slight variations. In brief, 100 μl of fresh BHI media was added to each set and the plates were then incubated. The media was renewed every 24 hours if needed. To obtain OD_{595} wells were washed gently twice with PBS. Next, CV (0.2%w/v) was added and allowed to sit for 5 min. After staining, the excess CV was removed, and wells were washed gently with PBS again to remove any remaining planktonic bacteria. The wells were then air-dried, and 33% glacial acetic acid was added to them in order to lyse all bacteria and remove excess CV. Finally, 200 μl aliquots were transfered into 96-well plates, and their OD_{595} was measured using a microtiter plate reader (iMark

Microplate Reader, Bio-Rad, USA). Figure 2.5 and 2.6 show CV assay experiments and 96 well-plates containing experimental groups before OD measurements respectively.

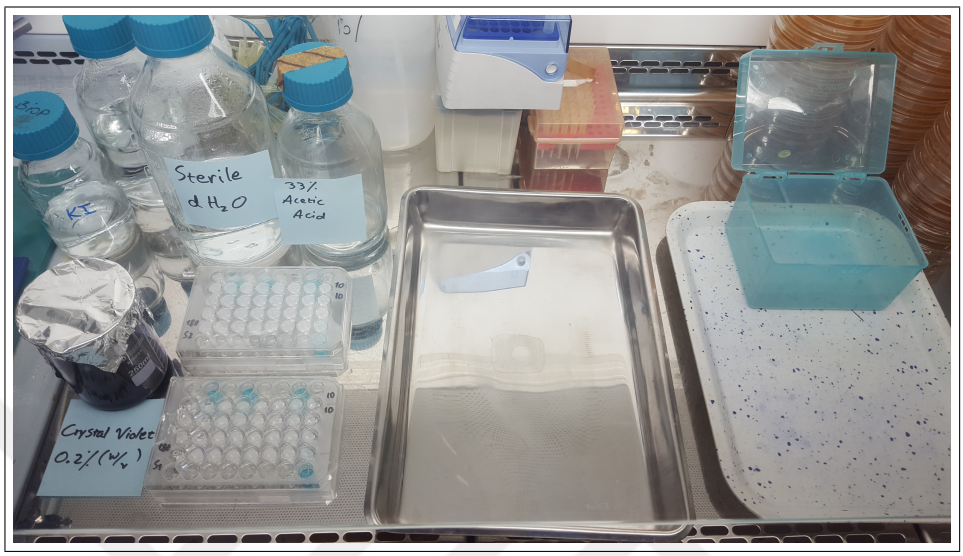

Figure 2.5 An image of CV assay procedure.

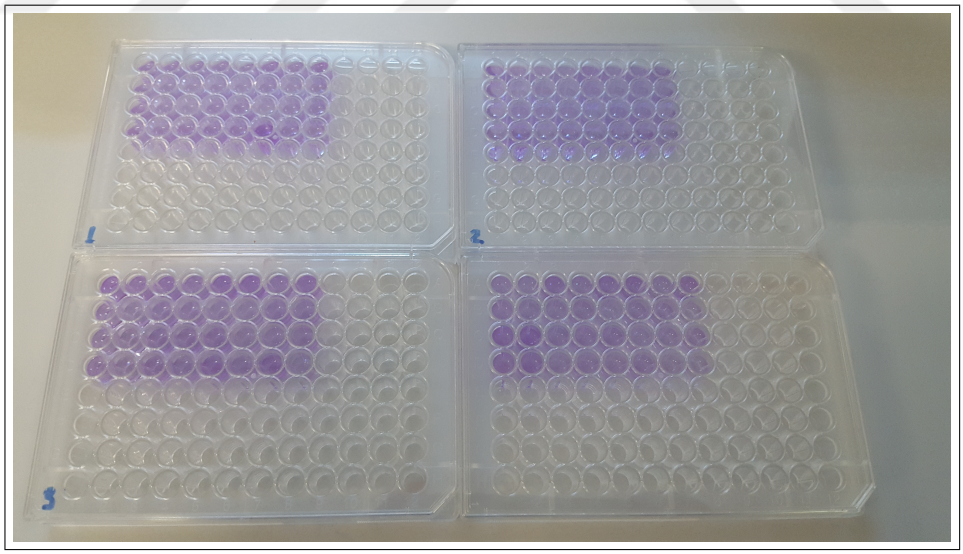

Figure 2.6 Experimental groups before OD_{595} measurement.

2.7 SEM visualisation of E.faecalis biofilms

SEM images were obtained to demonstrate the morphology of *E.faecalis* biofilms72 hours after aPDI treatments. General guidelines provided by Pourhajibagher et al. [39] were followed, with minor changes. In short, *E.faecalis* bacterial suspensions were grown at the bottom of 48-well Tissue Culture Plates (TCP). After 72 hours of growth, biofilms of groups G1, G7, and G8 were rinsed with sterile PBS and washed gently with sterile deionized water. The samples were then fixated by immersing the TCPs in 2.5% glutaraldehyde solution (Figure 2.7), followed by storing at 4 °C for 16 h. Afterwards, the plates were washed further with deionized water before being dehydrated by successive insertion in solutions containing 50% ,75% , and 100% ethanol respectively (Figure 2.8). After freeze drying for 1.5 h at -4 °C, the bottom of the respective wells were cut out, platinum sputtered (Figure 2.10), and then scanned with SEM (XL30 ESEM-FEG, PHILIPS) (Figure 2.11).

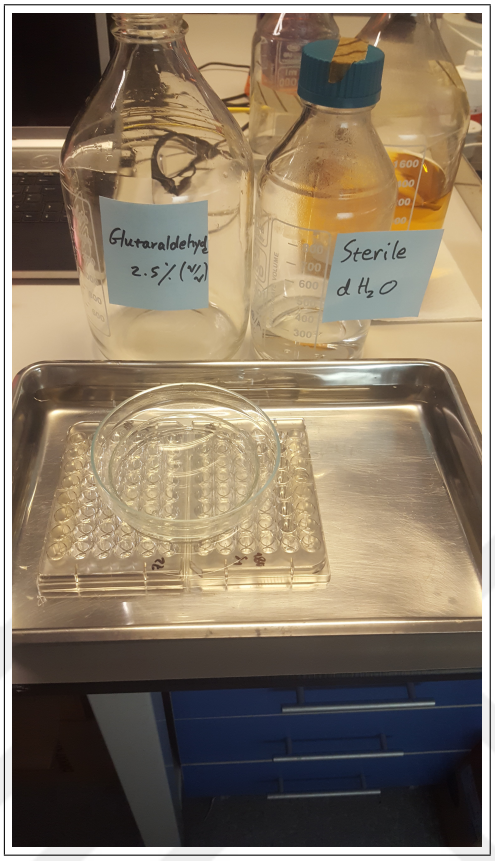

Figure 2.7 Sample fixation with 2.5% glutaraldehyde.

Figure 2.8 Sample dehydration by successive immersion in ethanol.

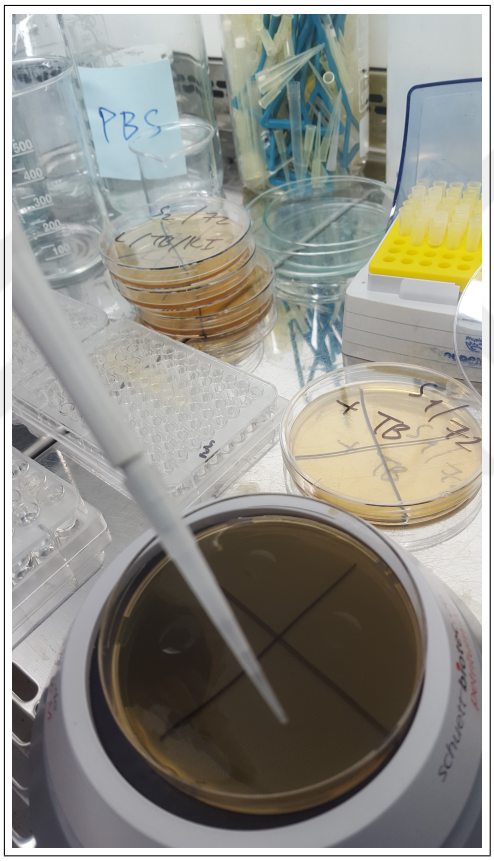

Figure 2.9 Plate spotting before CFU counting.

Figure 2.10 Platinum sputtering before SEM.

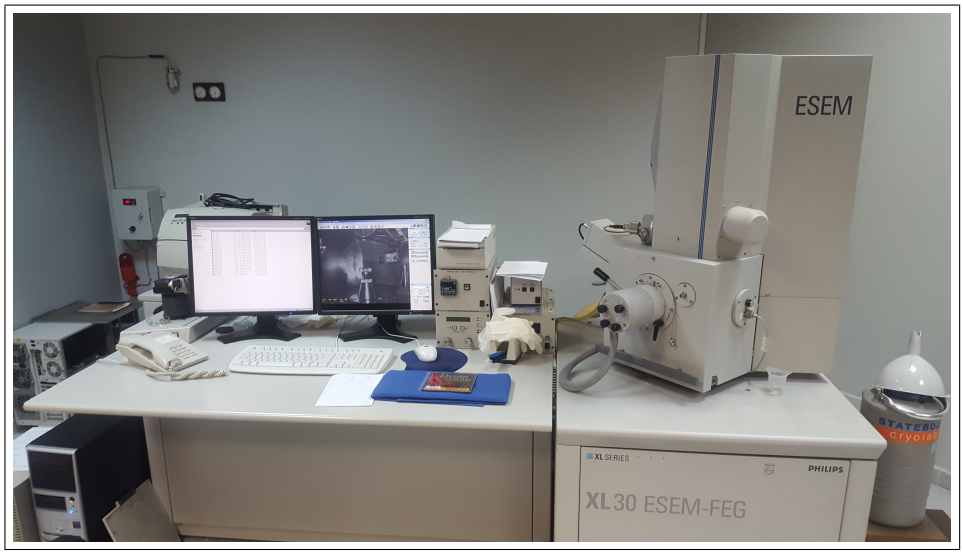

Figure 2.11 Image of SEM device used for biofilm visualisation.

2.8 Statistical Analysis

SPSS software version24 was used to analyze the CFU/ml (LOG10) data using analysis of variance (ANOVA) and Tukey's-b test. All experiments were performed at least three times, and the level of significance was selected at $p < 0.05$.

3. RESULTS

3.1 aPDI experiments

The CFU counts for all four concentration ranges showed decrease when normal PDT and potentiated PDT were compared with the control groups, but the extent of decrease changed significantly from CR1 to CR4 groups. More than 4 LOGS of photokilling was observed when aPDI was potentiated using 10 μM TBO/10 mM KI, followed by 180s exposure time. The results are plotted in Figure 3.1 as LOG(10) of CFU/ml values for all experimental groups: All aPDI groups (G7,G8) showed significant decrease compared to their controls. However, there was no significant difference between non aPDI groups (G2-G6) and controls except for G3 group of CR3. This is due to dark toxicity effect of TBO at high concentrations. However, when 10 mM KI was used (CR4), there was no significant decrease for G4 group.

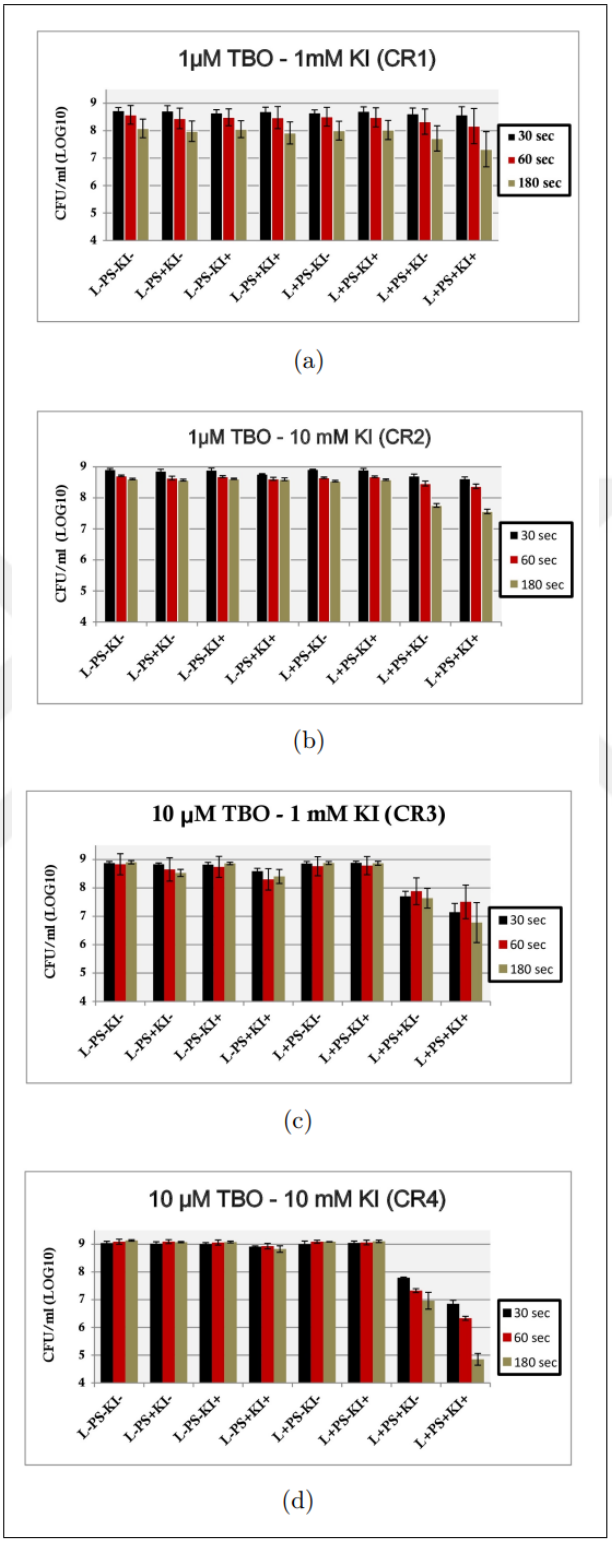

Figure 3.1 (a) aPDI experimental results for all groups (G1-G8) and Concentration Range CR1. (b) aPDI experimental results for all groups (G1-G8) and Concentration Range CR2. (c) aPDI experimental results for all groups (G1-G8) and Concentration Range CR3. (d) aPDI experimental results for all groups (G1-G8) and Concentration Range CR4.

3.2 Photothermal effect

Temperature variation profile with time was obtained for laser irradiation for 180 s and 300 mW power output. The results, shown in Figure 3.2 indicates an overall temperature increase of around 2 °C for the longest exposure time.

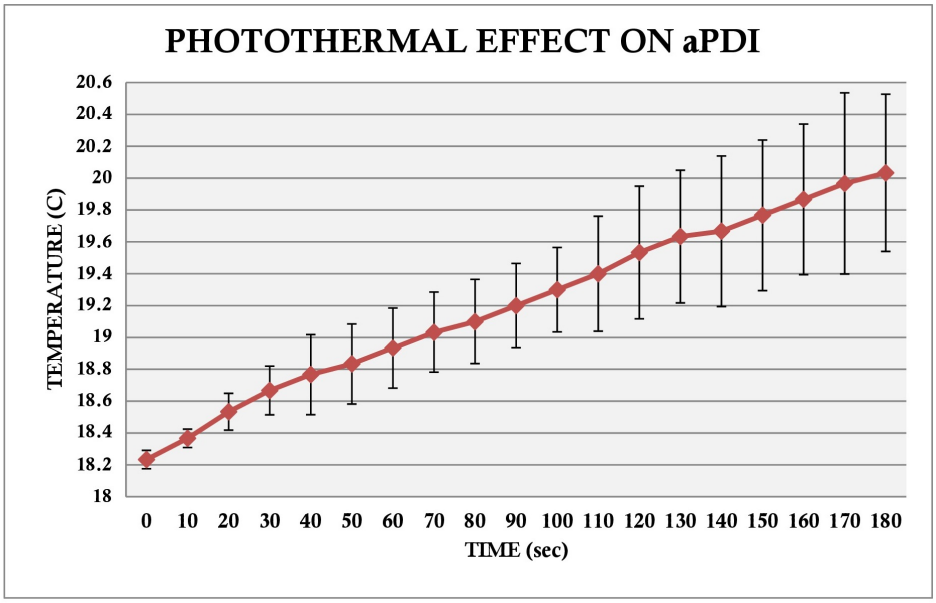

Figure 3.2 Photothermal effect on aPDI experiments.

3.3 Biofilm formation

Fig 3.3 shows the changes in CFU/ml (LOG10) and OD_{595} of G1,G7, and G8 groups at 24 h time intervals up to 72 hours after aPDI treatment.

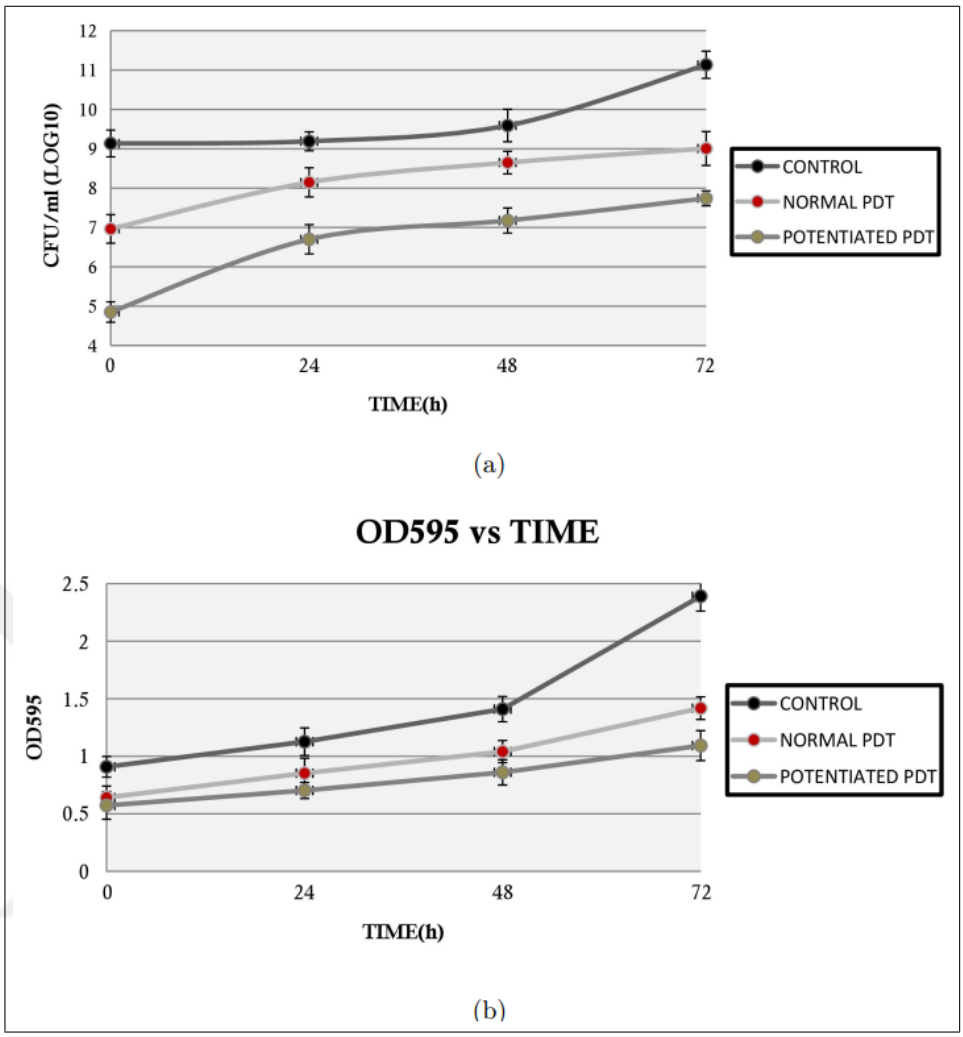

Figure 3.3 (a)Biofilm formation studies: Plot of CFU/ml (Log10) vs Time for G1, G7, and G8 groups. (b)Biofilm formation studies: Plot of OD595 vs Time for G1, G7, and G8 groups.

3.4 SEM micrographs of E.faecalis biofilms

The following real and SEM images, shown in Fig. 3.4, 3.5, and 3.6 were obtained (at 2000 and 5000 magnifications) for groups G1, G7, and G8 72 h post aPDI experiments to aid visualizing the extent of biofilm formation. Significant reduction of recurrent *E.faecalis* biofilm can be seen for PDT groups.

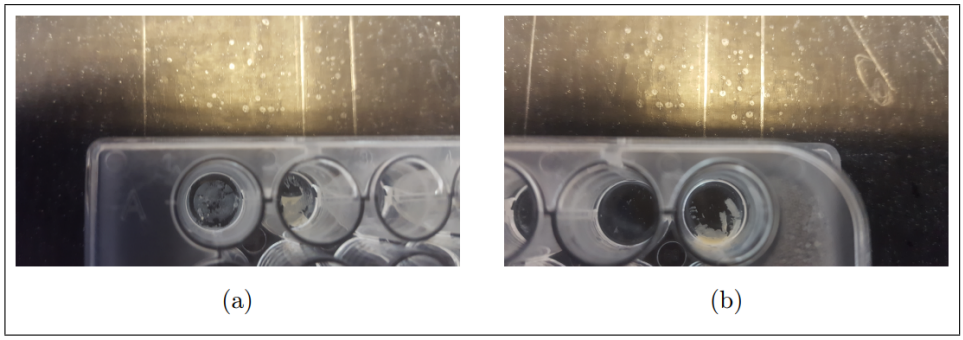

Figure 3.4 (a)Real image of experimental wells after biofilm analysis (control G1). (b)Real image of experimental wells after biofilm analysis (potentiated PDT G8).

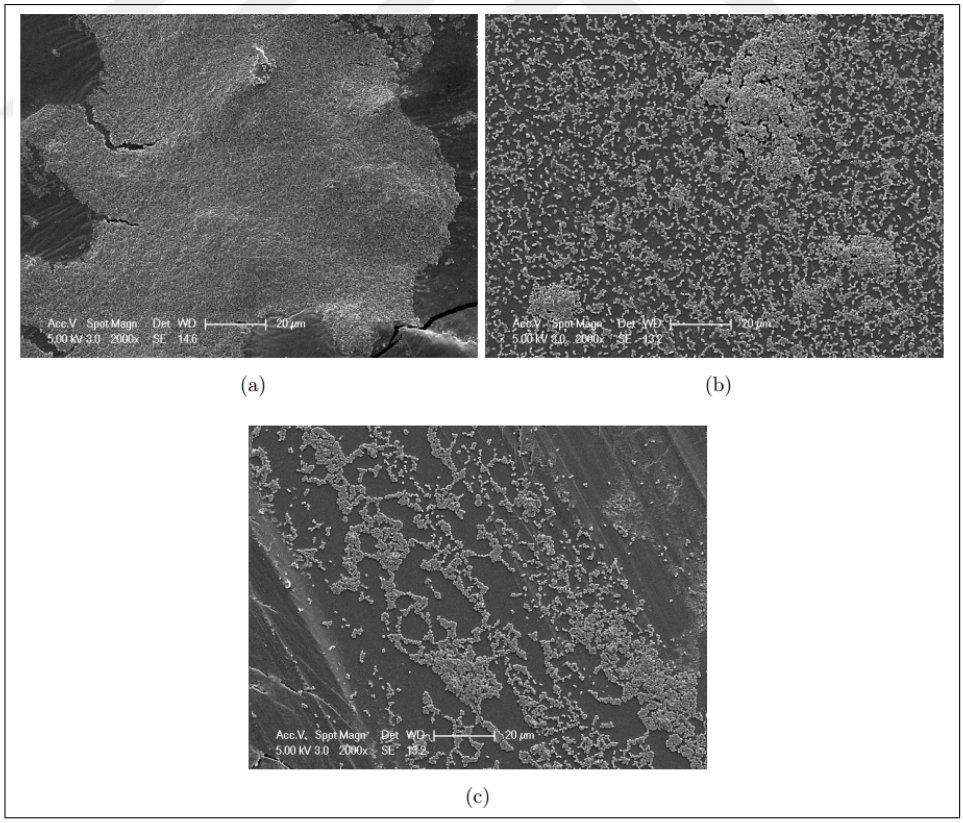

Figure 3.5 (a)SEM image of control (G1) (X2000). (b)SEM image of normal PDT (G7) (X2000). (c)SEM image of potentiated PDT (G8) (X2000).

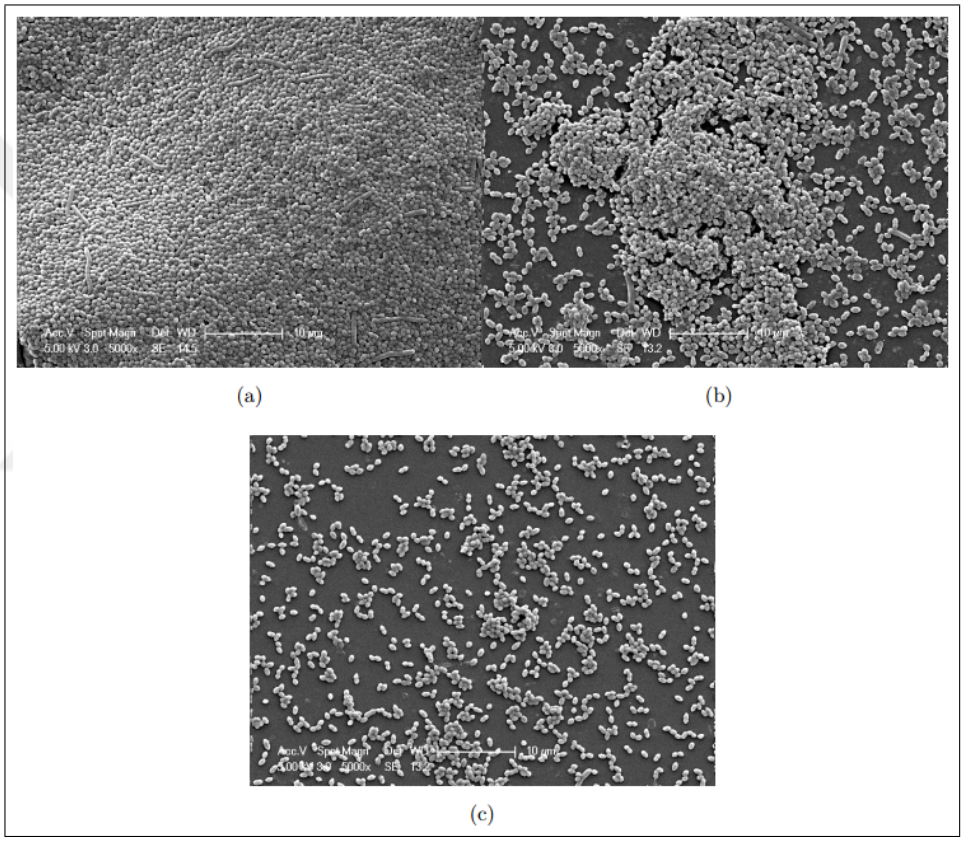

Figure 3.6 (a)SEM image of control (G1) (X5000). (b)SEM image of normal PDT (G7) (X5000). (c)SEM image of potentiated PDT (G8) (X5000).

3.5 Statistical analysis

No significant decrease was observed for experimental groups G2-G6 for all concentration ranges when compared to control ($p > 0.05$) , with the exception of CR3. But all G7 and G8 groups were significantly different with respect to control groups, and the significance level of CR3 and CR4 groups, for all exposure times, was calculated to be $p < 0.01$.

4. DISCUSSION

Normal aPDI results obtained in these studies match those of Giusti et al. [40]. In both studies, TBO concentrations in the range of few micromolars with similar fluence rates and up to 3 min of exposure reported an average 2 LOGS of killing. However, upon applying KI immediately before laser irradiation, the photokilling extent shows noticeable enhancement. The idea of potentiation by inorganic salts was first introduced by Hamblin et al. who used various concentration ranges of KI in conjunction with different PSs on different bacterial and fungal strains [41, 42]. It was proven that more than 6 LOGS of erradication could be achieved with KI concentrations as high as 100 mM for different bacterial strains.

Two major machanisms can be suggested as to how KI can reinforce aPDI action. First is the generation of **reactive iodine species**. Since TBO goes through type II mechanism of photodynamic action, the singlet oxygen present nearby iodide ions can initiate the following reaction:

$$^1O_2 + 3I^- + 2H_2O \longrightarrow I_3^- + 2H_2O_2 \tag{4.1}$$

The hydrogen peroxide produced in this reaction would undergo a series of other chain reactions, eventually yielding some other reactive species such as hydroxyl radicals, thereby enhancing the photodynamic effect [41]. The following chemical reactions indicate the pathway to formation of additional ROS:

$$I^- + 2H_2O_2 + H^+ \longrightarrow IOOH + 2H_2O \tag{4.2}$$

$$IOOH + I^- \longrightarrow HOOI_2^- \tag{4.3}$$

$$HOOI_2^- \longrightarrow I_2{}^{\bullet -} + HOO^{\bullet} \tag{4.4}$$

$$HOOI_2^- \longrightarrow I_2O^\bullet + OH^\bullet \tag{4.5}$$

Another proposed mechanism of action for aPDI enhancement by KI could be the **heavy atom effect**, which is defined as increase in the rate of spin-forbidden processes due to presence of an element with high atomic number. Iodine is a heavy atom, and since phenothiazinium dyes are reported to exhibit enhancement in the extent of their intersystem crossing due to internal heavy atom effect [43] (where a heavy atom is covalently attached to them), it is possible that external heavy atom effect (the case with I^- , which is freely available in the aquous media) would also contribute to increase in the rate of excited PS formation and enhance the aPDI effect. Recent studies have indicated that many classes of PSs can be synthetically designed and tuned via attachment of heavy atoms such as iodine and bromine in order to enhance the excitation energies by optimally adjusting the singlet-triplet energy gaps [44].

In case of photothermal effect, an average temperature increase of about 2 °C rules out the involvement of photothermal effect as a factor contributing to bacterial erradication, as the withering of *E.faecalis* does not start anywhere below 50 °C [45]. The reason why initial temperature starts at 18 °C is that the aPDI experiments were all performed under biosafety cabin.

Studies have confirmed that *enterococcal* biofilms are 10 to 1000 times harder to eliminate than planktonic ones [46]. *E.faecalis* is known predominantly as an invasive pathogen causing periodontitis and root canal infections, and many studies have addressed attempts to battle it using aPDI [26, 47]. But, *E.faecalis* is also an important pathogen affecting the urinary tract and is a common source of recurrent biofilm formation on urinary catheters [26]. One major side effect of employing ureteral stents is the encrustation ability of the bacteria already present in the urether. Thus, in searching for techniques that can potentially aid us combat the biofilm recurrence and encrustation, it is essential to analyse post-treatment biofilm formation capacity. Here we showed that the extent of biofilm formation following aPDI treatment possibly slows

down. Looking at the data provided in Figure 3.3 it can be proposed that for G7 and G8 groups, the normal transition from lag phase to exponential growth phase observed in G1 shows different behavior, plateauing at around 72 h. This can suggest that following aPDI, the rate of post-treatment biofilm recurrence would be less than that of non aPDI treated groups. However, further studies on this topic should be planned for near future in order to monitor the recurrence rate at greater lengths to obtain a more reliable post-treatment biofilm formation profile. A schematic of typical bacterial growth phase diagram can be seen in Figure 4.1 in order to give a better comparative measure of the post-treatment biofilm formation trends between the treated (G7,G8) and control (G1) groups.

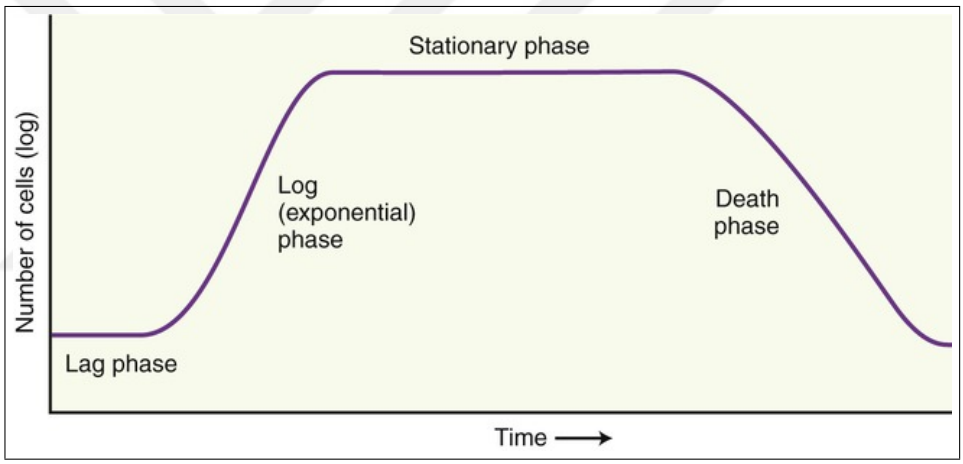

Figure 4.1 Schematic of Bacterial growth phases [48].

Bacterial biofilms on indwelling devices and implants are a significant problem throughout medicine [46], causing dangerous local and systemic infections resulting in significant morbidity and even death of the patient. 30% of the biofilm forming bacteria grow on indewelling medical devices [47], and among those, *E.faecalis* is a major bacteria that forms biofilm on urinary catheters [26]. Given the significant resistance of bacterial biofilms to antimicrobial agents, they are extremely difficult to treat and eradicate. At present, the only option to eliminate them is the replacement of the medical device, which often needs repeated surgical procedures which add significant morbidity to the patient and are costly to healthcare systems. While some research has gone into

eliminating already established biofilm, this has been very difficult to achieve given the complex structures of the biofilm. The most efficient treatment of biofilms would therefore be to prevent their formation in the first place by preventing initial bacterial adhesion to the material surface.With this in mind, the ability of aPDI to decrease bacterial biofilm formation by decreasing the initial bacterial load was tested. For this, a relatively high bacterial concentration was subjected to aPDI for varying periods of time followed by quantification of biofilm formation using a conventional TCP biofilm model. As shown in Figure 3.3, exposure of the bacterial cultures to aPDI for 180 s resulted in a significant decrease in bacterial numbers. Furthermore, the OD_{595} data show that this decrease in bacterial numbers resulted in decreased bacterial biofilm formation over a 72 hour period. This is also supported by the SEM data, which clearly show a less developed biofilm on the material surface for the samples treated with potentiated PDT. While this treatment did not prevent complete biofilm formation, it did provide proof of concept data that shows significant potential for the technology to prevent bacterial adhesion and biofilm formation. Additional experiments studying the effect of varying exposure time points as well as the effects on pre-formed biofilms are warranted to study the antimicrobial potential of this technology further.

5. CONCLUSION AND FUTURE WORK

Antimicrobial PDI using TBO as photosensitizer and KI as potentiator can significantly decrease the extent of surviving *E.faecalis* bacterial strains, with the highest photokilling being observed at 10 μM TBO/10 mM KI for 180 s irradiation time. Also, reduced rate of recurrent biofilm formation was observed for treatment groups compared to the control counterparts. The results of biofilm studies done at the end of PDT experiments were submitted for a journal publication at the end of project [49]. This thesis work also resulted in another publication by the Biophotonics lab [36]

This master's thesis Project offered significant results in reduction of CFU counts of *E.faecalis* bacterial strain as well as post-treatment quantification and observation of bacterial biofilms. However, it did not escape the author's mind that the static nature of these experimental setups are not in realistic accordance with how bacterial communities dwell, flourish, and form sessile matrices in biological environments. Therefore, if a research plan is to be devised in order to have experimental setups that mimic real behavior of infection-causing agents, the bacterial colonies must be grown and kept under constant flow of a fluid, which would render the bacterial mobility and subsequent biofilm formation conditions closer to reality. The effect of shear stress, the horizontal component of an external force exerted on a medium as a result of hydrodynamic pressure, should be accounted for since it determines the morphology and extent of heterogeneity of biofilm matrix [50]. Therefore, designing microfluidic systems that would allow growing biofilms in fluidic cells under constant liquid flow, coupled with real time and high resolution fluorescence imaging tools such as Confocal Laser Scanning Microscope (CLSM) [51] would facilitate a more comprehensive study scheme to better understand the Physics and Chemistry behind bacterial biofilm formation and growth. This would in turn give a rich, realistic, and valuable source of information to health professionals who are constantly working to resolve the ever increasing threat of infectious diseases.

REFERENCES

1. Miller-Keane, O. M., and M. T. O'Toole, "Miller-keane encyclopedia and dictionary of medicine, nursing, and allied health," *A Book. 7th ed. Philadelphia: Saunders*, 2003.

2. Hale, W. G., J. Margham, and V. A. Saunders, *Collins dictionary of biology*, Harpercollins Pub Ltd, 1995.

3. Van Boeckel, T. P., S. Gandra, A. Ashok, Q. Caudron, B. T. Grenfell, S. A. Levin, and R. Laxminarayan, "Global antibiotic consumption 2000 to 2010: an analysis of national pharmaceutical sales data," *The Lancet Infectious Diseases*, Vol. 14, no. 8, pp. 742–750, 2014.

4. Zaman, S. B., M. A. Hussain, R. Nye, V. Mehta, K. T. Mamun, and N. Hossain, "A review on antibiotic resistance: Alarm bells are ringing," *Cureus*, Vol. 9, no. 6, 2017.

5. Balsalobre, L. C., M. Dropa, and M. H. Matté, "An overview of antimicrobial resistance and its public health significance," *Brazilian Journal of Microbiology*, Vol. 45, no. 1, pp. 1–6, 2014.

6. Ventola, C. L., "The antibiotic resistance crisis: part 1: causes and threats," *Pharmacy and Therapeutics*, Vol. 40, no. 4, p. 277, 2015.

7. "Mechanisms of antibiotic resistance by bacteria,thermo fisher scientific,"https://www.thermofisher.com/blog/behindthebench/antibiotics-in-our-water-supply-are-we-polluting-the-element-of-life/", may02, 2018,"

8. Fischer, E., and V. Braun, "Permeability barrier of bacterial cell envelopes as cause of resistance to antibiotics (author's transl)," *Immunitat und Infektion*, Vol. 9, no. 3, pp. 78–87, 1981.

9. Munita, J. M., and C. A. Arias, "Mechanisms of antibiotic resistance," *Microbiology Spectrum*, Vol. 4, no. 2, 2016.

10. Webber, M., and L. Piddock, "The importance of efflux pumps in bacterial antibiotic resistance," *Journal of Antimicrobial Chemotherapy*, Vol. 51, no. 1, pp. 9–11, 2003.

11. De Pascale, G., and G. D. Wright, "Antibiotic resistance by enzyme inactivation: from mechanisms to solutions," *Chembiochem*, Vol. 11, no. 10, pp. 1325–1334, 2010.

12. "Molecular orbital diagrams for triplet and singlet oxygen, wikimedia commons, "https://commons.wikimedia.org/wiki/file:o2-states.svg", may03, 2018,"

13. Huang, L., Y. Xuan, Y. Koide, T. Zhiyentayev, M. Tanaka, and M. R. Hamblin, "Type i and type ii mechanisms of antimicrobial photodynamic therapy: An in vitro study on gram-negative and gram-positive bacteria," *Lasers in Surgery and Medicine*, Vol. 44, no. 6, pp. 490–499, 2012.

14. "Jablonski diagram for a conventional pdt procedure, "https://www.degruyter.com/view/j/nanoph.2017.6.issue-5/nanoph-2016-0189/nanoph-2016-0189.xml",hamblin et al. "advances in antimicrobial photodynamic inactivation at the nanoscale". nanophotonics, may03, 2018,"

15. Huang, L., T. Dai, and M. R. Hamblin, "Antimicrobial photodynamic inactivation and photodynamic therapy for infections," in *Photodynamic Therapy*, pp. 155–173, Springer, 2010.

16. F Sperandio, F., Y.-Y. Huang, and M. R Hamblin, "Antimicrobial photodynamic therapy to kill gram-negative bacteria," *Recent Patents on Anti-Infective Drug Discovery*, Vol. 8, no. 2, pp. 108–120, 2013.

17. Sridharan, G., and A. A. Shankar, "Toluidine blue: A review of its chemistry and clinical utility," *Journal of Oral and Maxillofacial Pathology: JOMFP*, Vol. 16, no. 2, p. 251, 2012.

18. "Chemical structure of toluidine blue ortho (tbo), "https://www.carlroth.com/en/en/life-science/histology-microscopy/staining-solutions/chromogenic-dyes/toluidine-blue-o-2018,"

19. Kasimova, K. R., M. Sadasivam, G. Landi, T. Sarna, and M. R. Hamblin, "Potentiation of photoinactivation of gram-positive and gram-negative bacteria mediated by six phenothiazinium dyes by addition of azide ion," *Photochemical & Photobiological Sciences*, Vol. 13, no. 11, pp. 1541–1548, 2014.

20. Hamblin, M. R., "Potentiation of antimicrobial photodynamic inactivation by inorganic salts," *Expert Eeview of Anti-Infective Therapy*, Vol. 15, no. 11, pp. 1059–1069, 2017.

21. Lee, H.-J., S.-M. Kang, S.-H. Jeong, K.-H. Chung, and B.-I. Kim, "Antibacterial photodynamic therapy with curcumin and curcuma xanthorrhiza extract against streptococcus mutans," *Photodiagnosis and Photodynamic Therapy*, Vol. 20, pp. 116–119, 2017.

22. Costa, R. O., P. M. d. Macedo, A. Carvalhal, and A. R. Bernardes-Engemann, "Use of potassium iodide in dermatology: updates on an old drug," *Anais Brasileiros de Dermatologia*, Vol. 88, no. 3, pp. 396–402, 2013.

23. Rosen, E., I. Tsesis, S. Elbahary, N. Storzi, and I. Kolodkin-Gal, "Eradication of enterococcus faecalis biofilms on human dentin," *Frontiers in Microbiology*, Vol. 7, p. 2055, 2016.

24. Prażmo, E. J., R. A. Godlewska, and A. B. Mielczarek, "Effectiveness of repeated photodynamic therapy in the elimination of intracanal enterococcus faecalis biofilm: an in vitro study," *Lasers in Medical Science*, Vol. 32, no. 3, pp. 655–661, 2017.

25. López-Jiménez, L., E. Fusté, B. Martínez-Garriga, J. Arnabat-Domínguez, T. Vinuesa, and M. Viñas, "Effects of photodynamic therapy on enterococcus faecalis biofilms," *Lasers in Medical Science*, Vol. 30, no. 5, pp. 1519–1526, 2015.

26. Flores-Mireles, A. L., J. N. Walker, A. Potretzke, H. L. Schreiber, J. S. Pinkner, T. M. Bauman, A. M. Park, A. Desai, S. J. Hultgren, and M. G. Caparon, "Antibody-based therapy for enterococcal catheter-associated urinary tract infections," *MBio*, Vol. 7, no. 5, pp. e01653–16, 2016.

27. Ding, K., Y.-W. Zhang, W. Si, X. Zhong, Y. Cai, J. Zou, J. Shao, Z. Yang, and X. Dong, "Zinc (ii) metalated porphyrins as photothermogenic photosensitizers for cancer photodynamic/photothermal synergistic therapy," *ACS Applied Materials & Interfaces*, 2017.

28. Sun, J., Y. Guo, R. Xing, T. Jiao, Q. Zou, and X. Yan, "Synergistic in vivo photodynamic and photothermal antitumor therapy based on collagen-gold hybrid hydrogels with inclusion of photosensitive drugs," *Colloids and Surfaces A: Physicochemical and Engineering Aspects*, Vol. 514, pp. 155–160, 2017.

29. Fekrazad, R., F. Khoei, N. Hakimiha, and A. Bahador, "Photoelimination of streptococcus mutans with two methods of photodynamic and photothermal therapy," *Photodiagnosis and Photodynamic Therapy*, Vol. 10, no. 4, pp. 626–631, 2013.

30. Flemming, H.-C., T. R. Neu, and D. J. Wozniak, "The eps matrix: the house of biofilm cells," *Journal of Bacteriology*, Vol. 189, no. 22, pp. 7945–7947, 2007.

31. Høiby, N., T. Bjarnsholt, M. Givskov, S. Molin, and O. Ciofu, "Antibiotic resistance of bacterial biofilms," *International Journal of Antimicrobial Agents*, Vol. 35, no. 4, pp. 322–332, 2010.

32. Tennert, C., K. Feldmann, E. Haamann, A. Al-Ahmad, M. Follo, K.-T. Wrbas, E. Hellwig, and M. J. Altenburger, "Effect of photodynamic therapy (pdt) on enterococcus faecalis biofilm in experimental primary and secondary endodontic infections," *BMC Oral Health*, Vol. 14, no. 1, p. 132, 2014.

33. Delcaru, C., I. Alexandru, P. Podgoreanu, M. Grosu, E. Stavropoulos, M. C. Chifiriuc, and V. Lazar, "Microbial biofilms in urinary tract infections and prostatitis: etiology, pathogenicity, and combating strategies," *Pathogens*, Vol. 5, no. 4, p. 65, 2016.

34. Kawahara, T., H. Ito, H. Terao, M. Yoshida, and J. Matsuzaki, "Ureteral stent encrustation, incrustation, and coloring: morbidity related to indwelling times," *Journal of Endourology*, Vol. 26, no. 2, pp. 178–182, 2012.

35. "Image of biofilm encrusted j-j uretheral stent, "https://www.spandidos-publications.com/maintenance.html",may03, 2018,"

36. Ghaffari, S., A. S. K. Sarp, M. K. Ruhi, and M. Gülsoy, "Antimicrobial blue light inactivation of neisseria gonorrhoeae," in *Light-Based Diagnosis and Treatment of Infectious Diseases*, Vol. 10479, p. 1047914, International Society for Optics and Photonics, 2018.

37. Garcez, A. S., S. C. Núnez, N. Azambuja Jr, E. R. Fregnani, H. M. Rodriguez, M. R. Hamblin, H. Suzuki, and M. S. Ribeiro, "Effects of photodynamic therapy on gram-positive and gram-negative bacterial biofilms by bioluminescence imaging and scanning electron microscopic analysis," *Photomedicine and Laser Surgery*, Vol. 31, no. 11, pp. 519–525, 2013.

38. O'Toole, G. A., "Microtiter dish biofilm formation assay," *Journal of Visualized Experiments: JoVE*, no. 47, 2011.

39. Pourhajibagher, M., E. Boluki, N. Chiniforush, B. Pourakbari, Z. Farshadzadeh, R. Ghorbanzadeh, M. Aziemzadeh, and A. Bahador, "Modulation of virulence in acinetobacter baumannii cells surviving photodynamic treatment with toluidine blue," *Photodiagnosis and Photodynamic Therapy*, Vol. 15, pp. 202–212, 2016.

40. Giusti, J. S., L. Santos-Pinto, A. C. Pizzolito, K. Helmerson, E. Carvalho-Filho, C. Kurachi, and V. S. Bagnato, "Antimicrobial photodynamic action on dentin using a light-emitting diode light source," *Photomedicine and Laser Surgery*, Vol. 26, no. 4, pp. 281–287, 2008.

41. Huang, L., G. Szewczyk, T. Sarna, and M. R. Hamblin, "Potassium iodide potentiates broad-spectrum antimicrobial photodynamic inactivation using photofrin," *ACS infectious Diseases*, Vol. 3, no. 4, pp. 320–328, 2017.

42. Zhang, Y., T. Dai, M. Wang, D. Vecchio, L. Y. Chiang, and M. R. Hamblin, "Potentiation of antimicrobial photodynamic inactivation mediated by a cationic fullerene by added iodide: in vitro and in vivo studies," *Nanomedicine*, Vol. 10, no. 4, pp. 603–614, 2015.

43. Rodriguez-Serrano, A., V. Rai-Constapel, M. C. Daza, M. Doerr, and C. M. Marian, "Internal heavy atom effects in phenothiazinium dyes: enhancement of intersystem crossing via vibronic spin–orbit coupling," *Physical Chemistry Chemical Physics*, Vol. 17, no. 17, pp. 11350–11358, 2015.

44. De Simone, B. C., G. Mazzone, N. Russo, E. Sicilia, and M. Toscano, "Excitation energies, singlet–triplet energy gaps, spin–orbit matrix elements and heavy atom effects in boimpys as possible photosensitizers for photodynamic therapy: a computational investigation," *Physical Chemistry Chemical Physics*, 2018.

45. Sörqvist, S., "Heat resistance in liquids of enterococcus spp., listeria spp., escherichia coli, yersinia enterocolitica, salmonella spp. and campylobacter spp," *Acta Veterinaria Scandinavica*, Vol. 44, no. 1, p. 1, 2003.

46. Percival, S. L., L. Suleman, C. Vuotto, and G. Donelli, "Healthcare-associated infections, medical devices and biofilms: risk, tolerance and control," *Journal of Medical Microbiology*, Vol. 64, no. 4, pp. 323–334, 2015.

47. Sayal, P., K. Singh, and P. Devi, "Detection of bacterial biofilm in patients with indwelling urinary catheters," *CIBTech J Microbiol*, Vol. 3, no. 3, pp. 9–16, 2014.

48. "Schematic of bacterial growth phases,"https://clinicalgate.com/bacteria-and-archaea/", may03, 2018,"

49. Ghaffari, S., A. S. K. Sarp, D. Lange, and M. Gülsoy, "Potassium iodide potentiated photodynamic inactivation of enterococcus faecalis using toluidine blue: Comparative analysis, and post-treatment biofilm formation study," *Photodyagnosis and Photodynamic Therapy*, Submitted on May 4, 2018.

50. Yawata, Y., J. Nguyen, R. Stocker, and R. Rusconi, "Microfluidic studies of biofilm formation in dynamic environments," *Journal of Bacteriology*, Vol. 198, no. 19, pp. 2589–2595, 2016.

51. Franklin, M. J., C. Chang, T. Akiyama, and B. Bothner, "New technologies for studying biofilms," *Microbiology Spectrum*, Vol. 3, no. 4, 2015.